Modification of electron density in F layer of ionosphere by dust suspension

M. S. Sodha[1,a)] and S. K. Mishra[2]
[1]*Centre for Energy Studies (CES), Indian Institute of Technology Delhi (IITD), New Delhi 110016, India*
[2]*ELI-ALPS, Szeged, Hungary*

(Received 21 February 2017; accepted 23 March 2017; published online 17 April 2017)

The effect of the suspension of high/low work function dust in the F layer ionospheric plasma has been investigated. On the basis of kinetics formulation of the F-layer dusty plasma, the local electron density is shown to reduce or enhance by inserting fine dust of appropriate physical/material properties. The formulation includes the number and energy balance of the plasma constituents along with the charging of the dust particles; a novel approach to investigate the effect of diffusion on plasma particles in the F-layer has been outlined. The consequence of the physical parameters of dust, namely, number density, material work function, photo-efficiency, and surface temperature, on the charging of dust and local plasma parameters at different ionospheric altitudes in the F layer has been worked out and presented graphically; the significance of plasma diffusion has been highlighted. The modification in local plasma density in the midday F-layer is seen to be sensitive to the dust parameters and altitude profile of the ionospheric plasma. Such modification in the local electron density is certainly of interest for radio wave propagation through the F layer. *Published by AIP Publishing*. [http://dx.doi.org/10.1063/1.4979988]

I. INTRODUCTION

There has been considerable interest in causing increase and decrease of electron density in the ionosphere with an aim to facilitate or disrupt electromagnetic (em) communications. Some of the applications[1,2] are over the horizon radar, L. F. Communication, H. F. ducted communication, and disabling/exploding space objects. Modification of electron density in the ionosphere may be realized[3] by the injection of chemicals, explosions, and heating by intense H.F. electromagnetic waves. There are three major facilities,[4] viz., HARP (USA) and TROMSO (Norway) located at polar latitudes and SURA (Russian Federation) at mid-latitudes, which are dedicated to the modification of electron density in the ionosphere by electromagnetic wave heating.

The fact that the electron density in a plasma can be decreased or increased by the suspension of dust of high or low (in the presence of low wavelength light) work function has been known[5–9] for quite some time. However, the concept was not explored in the context of the ionosphere till recently when Sodha *et al.*[10] computed the parameters of the ionospheric plasma with the suspension of low work function dust, corresponding to a height of 150 km. This exercise was primarily an illustration of the application of the formulation of kinetics of illuminated dusty plasma; the results obtained were only of qualitative significance, because the phenomenon of electron diffusion, which is significant at a height of 150 km or more (viz., F layer), was not included in the formulation of the kinetics. Misra and Mishra[11] made a steady state analysis of the kinetics of the E layer daytime plasma with a suspension of low/high work function dust; the formulation was based on the charge, number, and energy balance of the constituents and took into account a number of chemical/ionizing reactions. Srivastava *et al.*[12] considered the kinetics of an ideal Chapman α layer (specifically,[13,14] the ionospheric E layer at 105 km[14]) with a suspension of low/high work function dust. Electron diffusion[14] can be neglected in consideration of the E layer plasma (<150 km) but plays a prominent role in the kinetics of the F layer plasma. Since the major effort in ionospheric modification[4] has been concentrated on the F layer, we have explored in this paper the modification of the F layer electron density by the suspension of fine dust particulates. The methodology of the investigation consists of the following steps.

(*i*) Evaluation of the diffusion term in the continuity equation (or number balance) for a given spatial distribution $n_e(x)$ of electron density, in a form suitable for the study of kinetics; x is the ionospheric altitude. It is seen that the diffusion term can be reasonably well expressed as $D_a\lambda n_e(x)$, where λ is independent of x and $n_e(x)$ can be expressed as $n_e = n_1\exp(b_1x) + n_2\exp(-b_2x)$, where D_a is the ambipolar diffusion coefficient while λ is a parameter obtained from $n_e(x)$. (*ii*) From the number and energy balance of electrons and ions for the undisturbed (dust free) plasma as well as the electron temperature dependence of the electron-ion recombination coefficients, we obtain the number (per unit volume per unit time) and temperature of the electrons/ions, generated on account of the solar and cosmic flux of radiation and particles. This is required for the computation of λ, say, λ_0 for the undisturbed density distribution $n_{e0}(x)$, for the mid-latitudes midday F layer $\lambda_0 \approx 4.02\times10^{-6}\,\mathrm{km}^{-2}$. (*iii*) Writing the system of equations (number, energy. and charge balance) of the F layer plasma-dust suspension; the equations should include the diffusion term $D_a\lambda n_e$. (*iv*) These equations have been solved for λ and $n_e(x)$ by successive approximations, starting with $\lambda = \lambda_0$ and $n_e(x) = n_{e0}(x)$, the natural (without dust) electron density; these aspects are covered in Section II of this paper. Relevant parameters and computational scheme are described in Section III, while the

a)E-mail: msodha@rediffmail.com

numerical results based on the parametric analysis and the corresponding physical interpretation are given in Section IV. A summary of the outcome concludes this paper.

II. ANALYSIS

A. Ambipolar diffusion

The diffusion coefficient of the electrons (D_e) in the ionosphere is much larger than that of ions (D_i), and only little space charge is built up on account of the electrostatic force between the electrons and ions. Thus, the plasma diffuses as a whole with an ambipolar diffusion coefficient D_a. It may be shown that the diffusion term Λ in the continuity equation (number balance) is given by[13,15,16]

$$\Lambda = (D_a \sin^2 I)\left[\frac{d^2 n_e}{dx^2} + \frac{3}{2H}\frac{dn_e}{dx} + \frac{n_e}{2H^2}\right], \tag{1}$$

where $n_e(x)$ refers to the electron density at atmospheric altitude x and

$$H_r = kT_i/m_{0r}g, \tag{2}$$

with $\left[\overline{1/H}\right] = (g/kT_i)[\sum m_{0r}n_{0r}/\sum n_{0r}]$, k is Boltzmann's constant, T_i corresponds to the temperature of the ions, m_r refers to the mass of the ion of the rth variety, g is the acceleration due to gravity, $D_r = (kT_i/m_{0r}\nu_r)$, $\nu_r = \sum n_{0r}(3kT_i/m_{0r})^{1/2}Q_{0r}$, Q_{0r} and n_{0r} are the electron collision cross section and density associated with the neutral atom of the rth variety, and I is the inclination of the magnetic field; the computations refer to $I = \pi/2$. For the calculations, the diffusion term may further be simplified if the diffusion term (Eq. (1)) could be expressed as $D_a\lambda n_e$; with this simplification, the above equation reduces to

$$\Lambda = D_a\lambda n_e \Rightarrow \left[\frac{d^2 n_e}{dx^2} + \frac{3}{2H}\frac{dn_e}{dx} + \frac{n_e}{2H^2}\right] = \lambda n_e. \tag{3}$$

The solution of the above equation can be written as

$$n_e = n_1 \exp(bx) + n_2 \exp[-(b + 3/2H)x], \tag{4}$$

where $\lambda = b^2 + b(3/2H) + 1/2H^2$ and b is a constant which may be determined by using empirical fit to the ionospheric data.

The midday (midnight) data for mid-latitude ionospheric plasma have been tabulated by Gurevich,[17] which are used for the present calculations. Using the midday mid-latitude ionospheric data (for $H = 90$ km), one obtains $n_1 = 3.0044162 \times 10^7$/cc, $n_2 = -6.1939699 \times 10^7$/cc, and $b = -0.00641$/km, which may be used to obtain Λ from Eq. (3). The empirical fit for the altitude profile of the electron density in the F layer is displayed in Fig. 1; the fit for midnight data is not good. Furthermore, it should be mentioned that the plasma density $n_e(x)$ varies with time during the day (24 h) and thus the coefficient λ can also be expressed as a function of the time of day. The coefficient of ambipolar diffusion (D_a) along with the simplification $D_e \gg D_r$ can be written as[18]

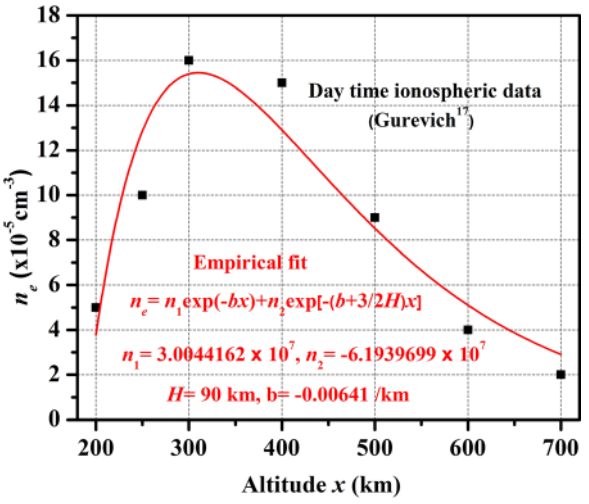

FIG. 1. Empirical fit for the electron density in the F-layer. The bold black dotted points refer to ionospheric data (Gurevich[17]) while the red color line corresponds to empirical fits.

$$D_a = [1 + (T_e/T_i)]/\sum D_r^{-1}(n_r/n_e). \tag{5}$$

In the F layer (~200–700 km), the ionic composition is dominated by the oxygen (O^+) ion (Table II of Ref. 17) and for weaker concentration of other ions, the ionospheric plasma is considered to be electrically neutral comprising electrons and singly charged oxygen ions along with neutral atoms/molecules with number density N_m and mass number equal to that of the dominant N_2 molecule (~28 amu). In this case, the coefficient of ambipolar diffusion (Eq. (5)) reduces to $D_a = [1 + (T_e/T_i)]D_i$.

B. Kinetics of undisturbed F layer ionospheric plasma

The ionospheric layer plasma primarily consists of electrons, multi species ions, and neutral species where the partial ionization is maintained by soft X-rays and UV solar radiation reaching the atmosphere; the plasma composition changes with change in neutral constituents in the atmosphere. For our analysis, the present study is confined to the F region plasma at an ionospheric altitude of ~200–700 km and midday time (mid-latitude noon) ionospheric structure specified by Gurevich;[17] the plasma constituents, ionic composition, and other relevant plasma parameters at different altitudes in the F–layer have been shown by Gurevich[17] (Tables I and II of his book). The plasma environment in the daytime is considered to be maintained on account of neutral ionization and various electron-ion recombination processes along with diffusion of plasma particles; it should be stated that the diffusion becomes less important at lower altitudes (<130 km) due to the abundance of electron collisions.[17] The ionospheric F–layer mainly comprises the neutral gas atoms/molecules of (O, O_2, N_2, and He) along with their respective ions ($O_2^+, O^+, N_2^+, NO^+, H^+, He^+$) and electrons; however, the ionization in the F region is dominated by the oxygen (O^+) ion. Considering the generation/annihilation and diffusion processes of electrons/ions, the kinetics equations describing the undisturbed F-region plasma can be written as follows.

1. Electron kinetics

$$(dn_{e0}/dt) = q_e - n_{e0}\sum \alpha_{r0} n_{ir0} + D_{a0}\lambda n_{e0}. \tag{6a}$$

2. Ions kinetics (rth ion)

$$(dn_{ir0}/dt) = q_{ir} - \alpha_{r0} n_{e0} n_{ir0} + D_{a0}\lambda n_{ir0}. \tag{6b}$$

3. Energy kinetics of electrons

$$\frac{d}{dt}\left(\frac{3}{2}n_{e0}kT_{e0}\right) = \left[q_e\left(\frac{3}{2}kT_{ge}\right) - n_{e0}\sum \alpha_{r0} n_{ir0}\left(\frac{3}{2}kT_{e0}\right)\right] + D_{a0}\lambda n_{e0}\left(\frac{3}{2}kT_{e0}\right). \tag{6c}$$

4. Energy kinetics of ions

$$\frac{d}{dt}\left[\left(\frac{3}{2}kT_{i0}\right)\sum n_{ir0}\right] = \left[\left(\frac{3}{2}kT_{gi}\right)\sum q_{ir} - n_{e0}\sum \alpha_{r0} n_{ir0}\left(\frac{3}{2}kT_{i0}\right)\right] + \left[D_{a0}\lambda \sum n_{ir0}\right]\left(\frac{3}{2}kT_{i0}\right), \tag{6d}$$

where q_e and q_{ir} are the rates of generation of electrons and ions of the rth variety, $\alpha_r = \alpha_{ro}(T_e/250)^{-\kappa}$ is the coefficient of recombination of electrons with ionic specie of the rth variety, while T_e and T_i refer the temperature of electrons and ions, respectively; the additional subscript 0 infers the parameters corresponding to the undisturbed plasma. Further considering the large heat capacity of neutral species and efficient energy exchange in collisions with ions, the neutral temperature (T_0) is considered to be constant at any given altitude. The above set of equations (Eq. (6)) is utilized to evaluate the coefficients q_e, q_{ir}, T_{ge}, and T_{gi} for the known altitude profile of the electron/ion density and temperatures in the undisturbed F ionospheric region; these parameters are necessary inputs in the kinetics of the ionospheric plasma in the presence of dust particles, discussed next.

C. Kinetics of F layer ionospheric plasma with dust particles

In order to understand the effect of fine particulates on F region phenomena, the kinetics of the complex F layer plasma comprising uniformly dispersed sub-micron spherical fine dust particles has been developed. The presence of fine dust particles stimulates the processes of the electrons/ions accretion on and photoemission (due to solar radiation) from the surface, resulting in charging of dust particles. These mechanisms along with other plasma processes (electron/ion generation/annihilation) have been used in writing the kinetics equations describing the number and energy balance of the plasma constituents.[10] For the sake of simplicity, in the analysis we have considered the constancy of neutral gas density (n_0); it is a justified assumption based on low ionization (n_i/n_0) in the F layer plasma. Again considering the large heat capacity of the neutral atoms/molecules and fine dust particles, their temperatures (T_0 and T_{d}, respectively) are considered to be constant in the present analysis. Following recent studies,[19–21] the basic equations governing the kinetics of dust particles in the F layer ionospheric plasma can be expressed as follows.

1. Charging of dust particles

The dust particles acquire charge on account of balance of electron and ion flux over the dust surface and the time evolution of dust charge can be expressed as[11]

$$(dz/dt) = n_{ph} + \sum n_{irc} - n_{ec}, \tag{7}$$

where n_{ph} is the photoemission current, n_{ec} is the electron accretion current, while n_{irc} corresponds to the ion accretion current associated with ions of the rth variety, and ze is the charge on dust particle.

2. Number balance

Considering different mechanisms of the electron/ion generation and annihilation, the time evolution of electron and ion densities can be written as[11]

Electron kinetics

$$(dn_e/dt) = \left[q_e - n_e\sum \alpha_r n_{ir} + D_a\lambda n_e\right] - n_d(n_{ec} - n_{ph}). \tag{8a}$$

Ions kinetics (*rth variety*)

$$(dn_{ir}/dt) = (q_{ir} - \alpha_r n_e n_{ir} + D_a\lambda n_{ir}) - n_d n_{irc}, \tag{8b}$$

and inherent charge neutrality

$$zn_d = n_e - \sum n_{ir}. \tag{9}$$

The terms in the square brackets on the right hand side of Eqs. (8a) and (8b) correspond to the net gain in electron and ion densities due to the ionization of neutral species, electron-ion recombination, and electron/ion diffusion processes in the plasma. The last terms in both the equations refer to the loss in electron/ion density due to net flow of electron/ion flux over the dust particle surface. It is noted that the number balance equations (Eq. (8)) along with the charge balance equation (Eq. (7)) characterize the quasi-neutrality of the complex dusty plasma as an inherent feature, which can be written as Eq. (9).

3. Energy balance of electrons/ions

The processes involved in the generation/annihilation of electrons/ions cause the energy exchange between the plasma constituents. In particular, the mean energy of electrons and ions gets significantly affected on account of dust grains. Further, in writing the energy balance of electrons the energy exchange in elastic collisions is ignored due to the smallness of its magnitude in comparison to other terms. As

another simplification in this analysis, the temperature of various ionic species is considered to be the same (T_i). The energy balance equations for electrons and ions in reference to the corresponding number balance equations (i.e., Eqs. (8a) and (8b)) can be written as[10,11]

$$\frac{d}{dt}\left(\frac{3}{2}n_e kT_e\right) = \left[q_e\left(\frac{3}{2}kT_{ge}\right) - n_e\sum\alpha_r n_{ir}\left(\frac{3}{2}kT_e\right)\right] + D_a\lambda n_e\left(\frac{3}{2}kT_e\right) - n_d(n_{ec}\varepsilon_{ec} - n_{ph}\varepsilon_{ph}), \tag{10a}$$

$$\frac{d}{dt}\left[\left(\frac{3}{2}kT_i\right)\sum n_{ir}\right] = \left[\left(\frac{3}{2}kT_{gi}\right)\sum q_{ir} - n_e\sum\alpha_r n_{ir}\left(\frac{3}{2}kT_i\right)\right] - n_d\varepsilon_{ic}\sum n_{irc} + \left[D_a\lambda\sum n_{ir}\right]\left(\frac{3}{2}kT_i\right), \tag{10b}$$

where $\varepsilon_{ec}(\varepsilon_{ic})$ refer to the mean energy (far away from the dust surface) associated with the electrons (ions) accreting on the surface of the dust particles surface while ε_{ph} corresponds to the mean energy of photo-emitted electrons at a large distance from the surface of the dust grain.

The terms in the square brackets on the right hand side in Eqs. (10a) and (10b) refer to the power gained per unit volume by electrons through neutral ionization and electron-ion recombination in the plasma. The 2nd term in both the equations corresponds to the net energy flow via particle diffusion per unit time per unit volume. The last term corresponds to the net power loss due to net electron flux over dust grains. The set of kinetic equations (i.e., Eqs. (7)–(10)) along with appropriate expressions (given later in text) describes the time evolution of dust and plasma parameters self-consistently.

III. RELEVANT EXPRESSIONS AND COMPUTATIONAL SCHEME

A. Relevant expressions

1. Evaluation of photoemission rate and mean energy of electrons from spherical dust grain

The daytime ionospheric layer is illuminated by continuous solar radiation causing photoemission from the dust surface. Following Fowler's approach,[22] the photoemission flux from the spherical metallic particles due to continuous solar radiation spectrum can be expressed as[23]

$$n_{ph}(z-1) = \pi a^2\int_{\varepsilon_{\nu 0}}^{\varepsilon_{\nu m}}\chi(\varepsilon_\nu)\left[\psi(\xi, z\alpha_d)/\Phi(\xi)\right]dn_{inc} \quad (for\ z \geq 0), \tag{11a}$$

$$= \pi a^2\int_{\varepsilon_{\nu 00}}^{\varepsilon_{\nu m}}\chi(\varepsilon_\nu)dn_{inc} \quad (for\ z < 0), \tag{11b}$$

where $\psi(\xi, z\alpha_d) = \Phi(\xi - z\alpha_d) + z\alpha_d ln[1 + \exp(\xi - z\alpha_d)]$, $\varepsilon_{\nu 00}$ refers to the threshold photon energy of the incident radiation and corresponds to the work function (φ) of the dust material as $\varepsilon_{\nu 00} = \varphi$, $\varepsilon_{\nu 0} = \left(\varphi + ze^2/a\right)$, $\varepsilon_{\nu m}$ refers to the upper limit of the solar radiation spectrum, $\chi(\varepsilon_\nu)$ represents the photoelectric yield of dust, $\alpha_d = \left(e^2/akT_d\right)$, $\xi = (h\nu - \varphi)/kT_d$, and $\Phi(\mu) = \int_0^{\exp\mu}\left[\Omega^{-1}\ln(1+\Omega)\right]d\Omega$.

Here, dn_{inc} is the number of photons incident per unit area per unit time due to solar radiation, lying in the frequency range ε_ν to $(\varepsilon_\nu + d\varepsilon_\nu)$ and given by[23]

$$dn_{inc} = (r_s/r_d)^2\left(4\pi\varepsilon_\nu^2/c^2\right)(eh/300)^3[\exp(\varepsilon_\nu/kT_s) - 1]^{-1}d\varepsilon_\nu, \tag{12}$$

where $r_s(\approx 6.96\times10^{10}\,\text{cm})$ is the radius of the radiating surface of the sun and $r_d(\approx 1.45\times10^{13}\text{cm})$ refers to the mean distance between the sun and gas-dust ensemble in the F–layer; in the above expression, ε_ν is expressed in eV. For all practical purposes, the sun may be considered as a black body radiating at $T_s \approx 5800\,\text{K}$.

Following earlier analyses,[11] the mean energy associated with the photo-emitted electrons (at a large distance from the dust surface) can be expressed as

$$\left(\frac{\varepsilon_{ph}(z-1)}{kT_d}\right) = \left[\left(\frac{\pi a^2}{n_{ph}}\right)\int_{\varepsilon_{\nu 0}}^{\varepsilon_{\nu m}}\left(\frac{\chi(\varepsilon_\nu)}{\Phi(\xi)}\int_{z\alpha_d}^{\infty}y^2[1+\exp(y-\xi)]^{-1}dy\right)dn_{inc}\right] - z\alpha_d \quad for z > 0 \tag{13a}$$

and

$$= \left[\left(\frac{\pi a^2}{n_{ph}}\right)\int_{\varepsilon_{\nu 00}}^{\varepsilon_{\nu m}}\left(\frac{\chi(\varepsilon_\nu)}{\Phi(\xi)}\int_{0}^{\infty}y^2[1+\exp(y-\xi)]^{-1}dy\right)dn_{inc}\right] + z\alpha_d \quad for z \leq 0. \tag{13b}$$

For computations, the solar radiation flux lying within the range $0 < \varepsilon_\nu < 8.3\,\text{eV}$ (corresponding to a wavelength $\lambda > 150\,\text{nm}$) is considered as the source of electron photoemission from the dust particles. It is noticed that the photoemission rate and mean energy are significantly influenced by photoelectric efficiency of the dust material. For the analysis, Spitzer formulation[24] for the photo-efficiency spectral dependence is considered herein, which may be expressed as

$$\chi(\varepsilon_\nu) = (729\chi_m/16)(\varepsilon_{\nu 00}/\varepsilon_\nu)^4[1 - (\varepsilon_{\nu 00}/\varepsilon_\nu)]^2. \tag{14}$$

In the above expression, χ_m refers to the maximum value of the photo-efficiency.

2. Accretion rates of electrons/ions over dust particles and mean energy

Assuming the Maxwellian distribution of the ionospheric plasma particles in the F layer, the orbital motion

limited (OML) currents associated with the electrons/ions accreting over dust particles and corresponding mean energy may be expressed as[9]

$$\begin{aligned} for\ z \geq 0:\ n_{ec}(z) &= \pi a^2 (8kT_e/m_e\pi)^{1/2} n_e (1+z\alpha_e), \\ \varepsilon_{ec}(z) &= [(2+z\alpha_e)/(1+z\alpha_e)]kT_e, \\ n_{irc}(z) &= \pi a^2 (8kT_i/m_{ir}\pi)^{1/2} n_{ir} \exp(-z\alpha_i), \\ \varepsilon_{ic}(z) &= 2kT_i + \left(ze^2/a\right) \text{ and } \alpha_{e,i} = \left(e^2/akT_{e,i}\right), \end{aligned} \tag{15a}$$

$$\begin{aligned} for\ z < 0:\ n_{ec}(z) &= \pi a^2 (8kT_e/m_e\pi)^{1/2} n_e \exp(z\alpha_e), \\ \varepsilon_{ec}(z) &= 2kT_e - \left(ze^2/a\right), \\ n_{irc}(z) &= \pi a^2 (8kT_i/m_{ir}\pi)^{1/2} n_{ir} (1-z\alpha_i), \\ \varepsilon_{ic}(z) &= [(2-z\alpha_i)/(1-z\alpha_i)]kT_i. \end{aligned} \tag{15b}$$

B. Computational scheme and data

For a numerical appreciation of the analysis, the midday F region plasma at the ionospheric altitude (∼200–700 km from the earth surface, at 12:00 noon) has been considered for the computations; the altitude dependence of the ambient ionospheric plasma constituents, composition, and other relevant parameters are chosen from the book by Gurevich[17] and are given in Table I. For computations, the ionospheric plasma is considered to be comprised of electrons and dominant oxygen ions ($n_e \approx n_i$) along with uniformly dispersed submicron metallic particles with specific material characteristics; with this simplification, the kinetics equations (Eqs. (7)–(10)) reduce to the case of the complex plasma with a single ion specie. The effect of dust particles on the plasma features at different ionospheric altitudes in F layers has been analyzed on the basis of the uniform charge theory,[21] applicable to the uniform size dust grains. The continuous radiation spectrum ($0 < \varepsilon_\nu < 8.3$ eV) of the sun reaching near earth space (1AU) is considered to be responsible for the photoemission from dust particles while electron/ion collection over the grain surface is the additional charging mechanism taken into account. Using this formulation, the effect of dust grain parameters, e.g., work function ($\varphi \sim 1.5\,\text{V} - 8.0\,\text{V}$) and photo-efficiency ($\chi_m \sim 0.001 - 1$), on the F layer ionospheric plasma environment has been analyzed; three cases of the F region plasma comprising the dust particles of Cs coated bronze ($\varphi \sim 1.5$ V), LaB_6 ($\varphi \sim 2.5$ V), and CeO_2 ($\varphi \sim 4.7$ V) have specifically been explored. The mean surface temperature of the dust particles (T_d) in the ionosphere may be determined by equating the solar radiation absorption by the particle to the power lost by thermal radiation and neutral cooling. For the sake of convenience, in computations a typical value of dust temperature $T_d = 250$ K is taken into account; however, the effect of dust surface temperature on plasma features has also been explored.

The following set of standard parameters along with data listed in Table I has been used in computations; the effect of various parameters on the ionospheric plasma kinetics has been studied by varying one parameter and keeping others the same.

$T_s \approx 5800$ K, $T_d = 250$ K, $a = 100$ nm, $\chi_m = 1.0$, $m_i \approx m_p = 1.67 \times 10^{-24}$ g, $m_n \approx 28 m_p$, $m_{O^+} \approx 16 m_i$, $\alpha_O \sim 4.5 \times 10^{-7}$ cm^{-3}, and $\kappa \sim 0.7$.

Using the ambient plasma parameters with appropriate expressions, the steady state features of the ionospheric plasma can be obtained by the simultaneous solution of the set of differential Eqs. (7)–(10). Here, due to fast processes of electron/ion accretion on and electron emission from dust, the steady state is achieved in few (∼10 s) seconds, and hence, the effect of variation in the solar radiation flux in this duration is ignored in computations.

IV. NUMERICAL RESULTS AND DISCUSSION

An analytical model describing the kinetics of fine particles in the midday F–layer ionospheric plasma has been developed on the basis of the uniform charge theory. In this formulation, the number and energy balance of the plasma constituents along with electron/ion flux balance over dust have been taken into account. The plasma generation due to ionization of neutral species (primarily due to solar radiation or charge exchange), electron-ion recombination, electron/ion accretion on and photoelectron emission from dust particles are the mechanisms considered herein. In this formulation, a novel approach to include the plasma particle diffusion in the F-layer analysis is adopted; the diffusion term is proportional to $n_e(x)$ for a certain analytical functional dependence of $n_e(x)$, which is valid for the altitude profile of the F layer electron (ion) density. Due to this diffusion term, the electron/ion collection over the dust particle surface is anticipated to reduce and this may result in higher positive potential over the dust particles. Further, according to the electron density profile the magnitude of the electron/ion collection is expected to be large around ∼300 km and

TABLE I. Ionospheric F-layer plasma composition and other relevant parameters (Ref. 17).

Altitude (km)			200	250	300	400	500	600	700
Neutral (N_m)	Density (cm^{-3})		8.4×10^9	2.5×10^9	9.3×10^8	2.0×10^8	5.6×10^7	1.7×10^7	6.0×10^6
	Temp. T_0 (K)		1070	1250	1330	1390	1400	1400	1400
Electrons	Density (cm^{-3})		5.0×10^5	1.0×10^6	1.6×10^6	1.5×10^6	9.0×10^5	4.0×10^5	2.0×10^5
	Temp. T_e (K)		1300	1700	2000	2400	2600	2700	2800
Ions	Relative ionization	He^+	…	…	…	0.005	0.015	0.02	0.04
		N^+	0.005	0.006	0.01	0.02	0.06	0.08	0.10
		O^+	0.90	0.98	0.99	0.97	0.90	0.84	0.75
		H^+	…	…	…	0.01	0.03	0.06	0.11
	Temp. T_i (K)		1100	1300	1400	1450	1600	2100	2200

one can anticipate small positive potential near this altitude. Through numerical calculations in this analysis, we examine the effect of artificially inserted fine dust particles on electron-ion plasma density/temperature and dust particle electric potential variation at different ionospheric altitudes in the F–region plasma. The numerical results for transient/steady state dust surface potential and corresponding plasma density/temperature are shown in Figs. 2–8 and illustrated graphically as a function of ionospheric altitude x, n_d, φ, χ_m, and T_d.

The transient evolution of the surface potential, local electron density, and temperature corresponding to Cs coated bronze ($\varphi \sim 1.5$ V) and $n_d = 10\,\mathrm{cm}^{-3}$ at different atmospheric

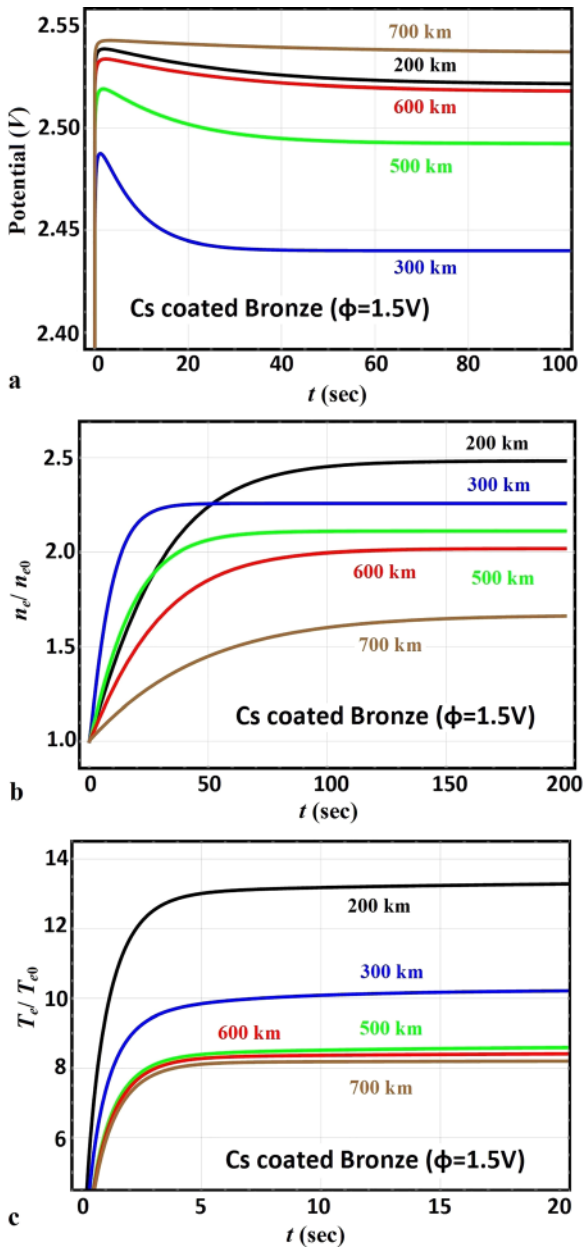

FIG. 2. Transient evolution of (a) the surface potential over dust particles, (b) dimensionless electron density (n_e/n_{e0}), and (c) dimensionless electron temperature (T_e/T_{e0}) for parameters $\varphi = 1.5$ V (Cs coated Bronze), $a_o = 0.1\,\mu$m, $T_d = 250$ K, $\chi_m = 1$, and $n_d = 10\,\mathrm{cm}^{-3}$; the curves correspond to different ionospheric altitudes in the F-layer and the parameters (n_e and T_e) are normalized with their magnitude at referred altitude.

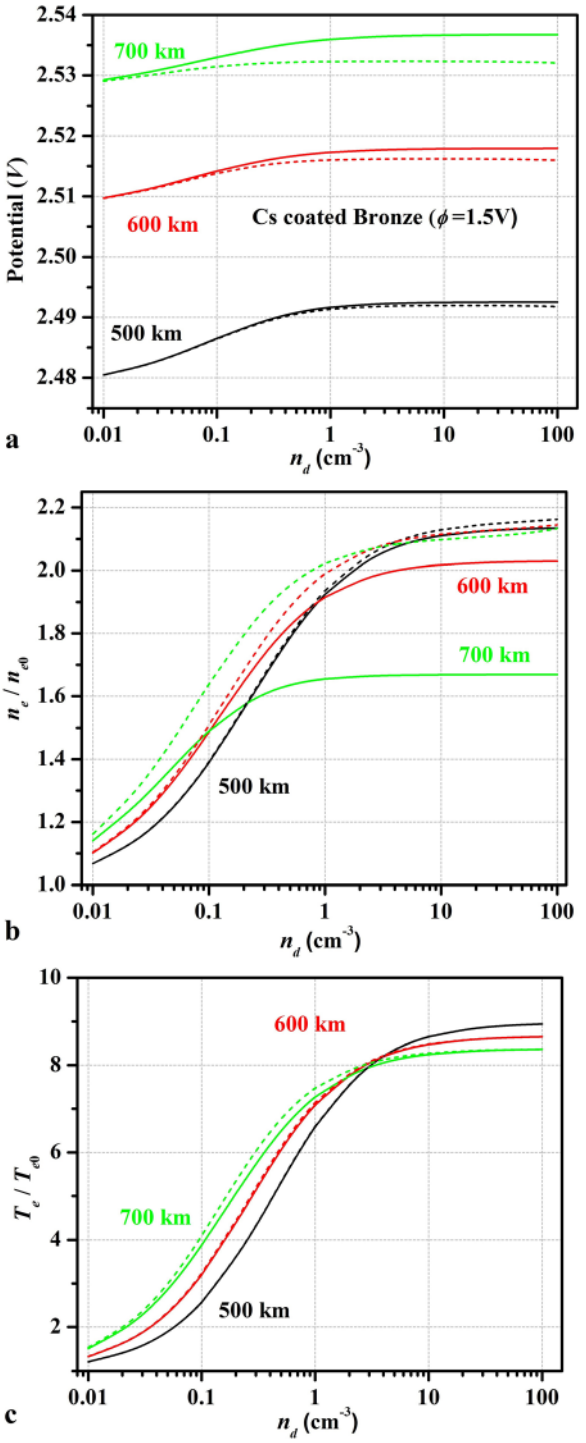

FIG. 3. Steady state dependence of (a) surface potential over dust particles, (b) dimensionless electron density (n_e/n_{e0}), and (c) dimensionless electron temperature (T_e/T_{e0}) on the number density (n_d) of the particles for parameters $\varphi = 1.5$ V (Cs coated Bronze), $a_o = 0.1\,\mu$m, $\chi_m = 1$, and $T_d = 250$ K; the curves correspond to different ionospheric altitudes in the F-layer and the parameters (n_e and T_e) are normalized with their magnitude at referred altitude. The broken and solid lines refer to the case where the diffusion term is ignored and included, respectively, in the calculations.

altitudes is illustrated in Fig. 2. The transient behaviour infers the characteristic time of achieving the steady state features; e.g., the charging time is noticed to be of the order of ∼40 s (Fig. 2(a)) while the electron density achieves a steady state in ∼200 s (Fig. 2(b)). The charging time is small enough in

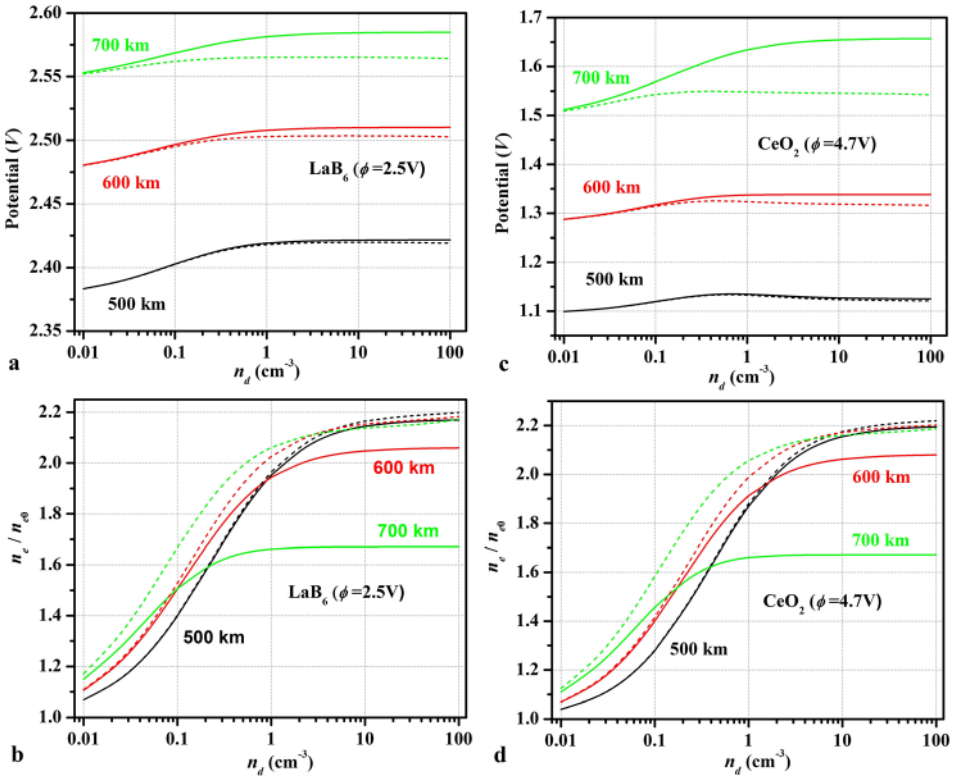

FIG. 4. Steady state dependence of (a) and (c) the surface potential and (b) and (d) the dimensionless electron density (n_e/n_{e0}) corresponding to LaB_6 ($\varphi = 2.5$ eV) and CeO_2 ($\varphi = 4.7$ eV), respectively, for $a_o = 0.1\,\mu$m, $\chi_m = 1$, and $T_d = 250$ K; the curves correspond to different ionospheric altitudes in the F-layer and the parameter (n_e) is normalized with its magnitude at referred altitude. The broken and solid lines refer to the case where the diffusion term is ignored and included, respectively, in calculations.

comparison to the solar cycle in a day and hence for a study of dependence of plasma parameters during the day, the use of steady state values is justified. The behaviour of the steady state magnitude of the dust surface potential (Fig. 2(a)) and electron density (Fig. 2(b)) is a consequence of the accretion current associated with the altitude profile of the electron/ion density while the electron temperature behaviour (Fig. 2(c)) may be primarily attributed to energy associated with electron emission by dust. The dependence of steady state surface potential and other plasma features (n_e/n_{e0} and T_e/T_{e0}) on the number density (n_d) of the dust particles at different ionospheric altitudes in the F-layer is illustrated in Fig. 3. The electric potential (Fig. 3(a)) over the dust surface is seen to increase with the increase in the number density of the dust particles; this nature may be the consequence of the balance of reduced electron/ion flux over dust particle due to the increase in diffusion flux with the photoemission flux at any given altitude. Further, the influence of the diffusion in the F layer on the electron density is shown in Fig. 3(b) where it is observed to decrease in the presence of particle diffusion and this difference, i.e., between the local plasma density in the presence and absence of diffusion term in the analysis increases with increasing ionospheric altitude; this ultimately affects the electron/ion current over the dust surface and hence the electric potential is shown to acquire higher positive potential (Fig. 3(a)) due to decreasing electron/ion accretion current in the presence of plasma diffusion. The ion density (n_i) can be evaluated by using the quasi-neutrality (Eq. (9)) of the dusty F layer along with charge and electron density (Figs. 3(a) and 3(b)) estimates. The mean electron temperature is seen to increase with the increase in n_d as illustrated in Fig. 3(c); this may be attributed to larger contribution in the plasma density via electrons associated with photo-emission flux. In calculations, the ion temperature is seen to be literally being unaffected ($T_i/T_{i0} \sim 1$) for the parameter range considered herein. Similar variations, viz., dust surface potential and local plasma density corresponding to LaB_6 ($\varphi \sim 2.5$ V, 4(a) and 4(b)) and CeO_2 ($\varphi \sim 4.7$ V, 4(c) and 4(d)) are illustrated in Fig. 4; the nature of the curves is similar to that obtained in the case of Cs coated bronze.

Fig. 5 illustrates the effect of varying work function of the dust material on the dust potential and other plasma features at different ionospheric altitudes in the F layer. The surface potential is seen to decay with increasing work function of the dust material (Fig. 5(a)) and consequently the electron density (Fig. 5(b)); this behaviour is primarily because of decay in photoemission current from the dust surface with increasing work function. It is noticed that the local plasma density may be enhanced 1.6–2.7 times than the ambient density by using a low work function (1.5 eV) dust. It is also observed that it is difficult to achieve electron bite out situation[21] (local electron density lower than the ambient value); however, this could be attained only for very high work function dust grains (~8 eV). The effect of the material work function on electron temperature (Fig. 5(c)) can be understood in terms of the electron density profile (Fig. 5(b)) where the significant fraction in the local plasma density comes through photoelectron flux. The photoelectric efficiency which describes the coupling of incident photon flux (solar radiation) with the dust surface is another crucial parameter. The effect of varying χ_m on the electron plasma density and dust surface potential at different ionospheric altitudes corresponding to moderate (4.7 eV, CeO_2) and high (8.0 eV) work function dust is displayed in Fig. 6. The surface potential (Fig. 6(a)) and consequent local plasma density (Fig. 6(b)) are observed to increase with increasing

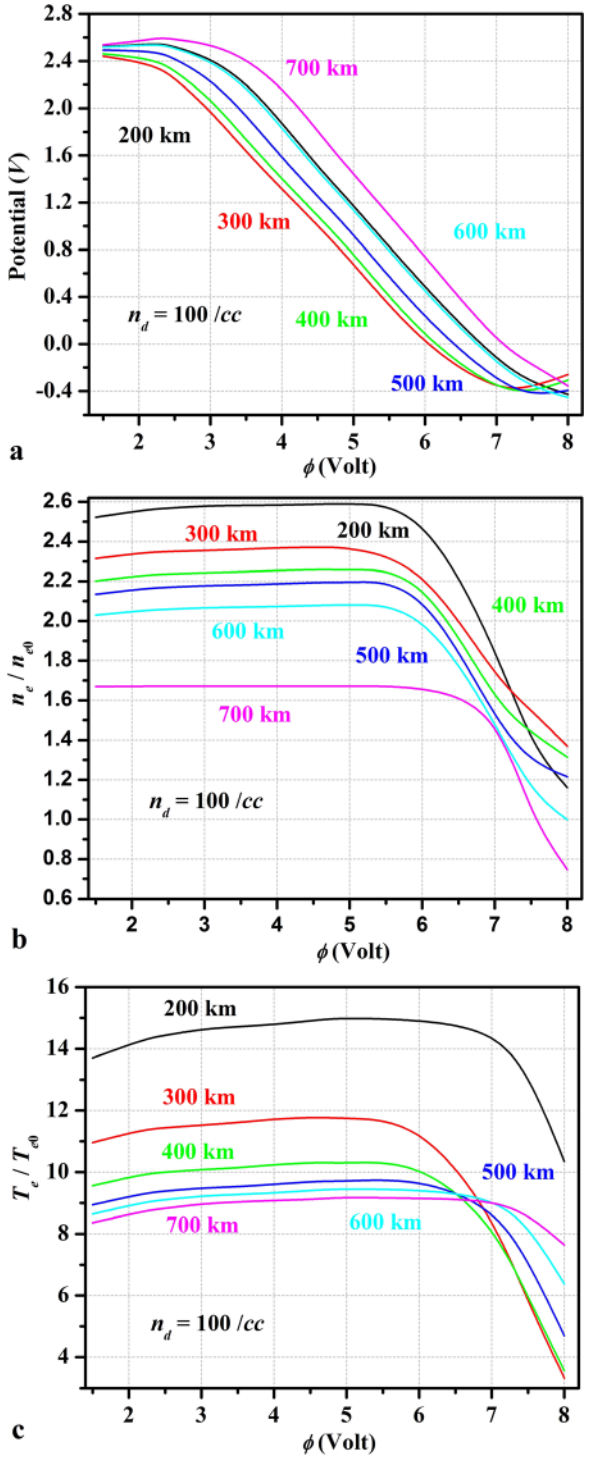

FIG. 5. Steady state dependence of (a) the surface potential over dust particles, (b) dimensionless electron density (n_e/n_{e0}), and (c) electron temperature (T_e/T_{e0}) on the work function of the dust material (φ) for the parameters $n_d = 100/\text{cc}$, $a_o = 0.1\,\mu\text{m}$, $\chi_m = 1$, and $T_d = 250\,\text{K}$; the curves correspond to different ionospheric altitudes in the F-layer and the parameter n_e is normalized with its magnitude at referred altitude.

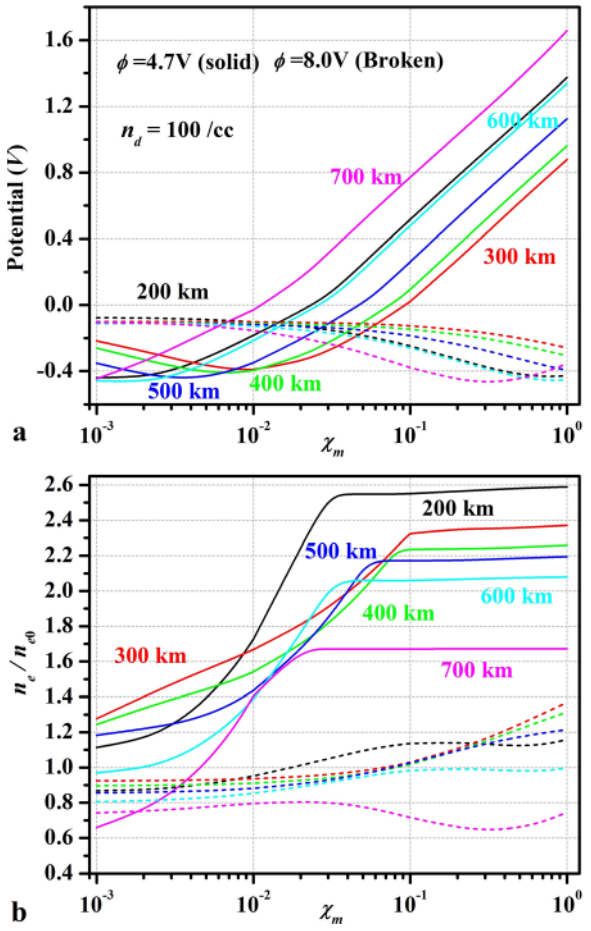

FIG. 6. Steady state dependence of (a) the surface potential over dust particles and (b) dimensionless electron density (n_e/n_{e0}) on the photoelectric efficiency of the dust particle material (χ_m) for the parameters $\varphi = 4.7\,\text{eV}$ (CeO_2, solid lines) and $\varphi = 8.0\,\text{eV}$ (pure ice, Broken lines), $n_d = 100/\text{cc}$, $a_o = 0.1\,\mu\text{m}$, and $T_d = 250\,\text{K}$; the curves correspond to different ionospheric altitudes in F-layer and the parameter n_e is normalized with its magnitude at referred altitude.

photoelectric yield (χ_m); this is primarily caused by the increase in photoemission flux with increasing χ_m. From the calculations, it is also noticed that the electron bite out scenario (reduction of plasma density from ambient) locally could be obtained by using low efficiency-high work function dust.

It is also interesting to point out that the dust surface temperature, which has arbitrarily been taken $T_d \sim 250\,\text{K}$ in calculations, may also vary depending on the surrounding physical environment and surface material itself. The effect of varying dust temperature on the surface potential and consequent plasma density is shown in Fig. 7. Higher surface temperature increases the number of electrons in statistical distribution inside the surface available for the emission; this might result in increasing photoelectron flux. In the case of moderate work function dust (4.7 eV, CeO_2), the surface potential is noticed to increase with the increase in the surface temperature as anticipated while the local plasma density is noticed to literally remain constant for the present set of parameters. On the other hand, in the case of high work function dust (8.0 eV) the potential and consequent plasma density are observed to decrease with T_d. The reduction of the local plasma electron density is noticed with the increase in dust surface temperature. The altitude dependence (x) of the dust surface potential (Fig. 8(a)) and corresponding plasma density (normalized with respective unperturbed plasma density, Fig. 8(b)) for the different material work functions (4.7 eV and 8.0 eV) and dust density (n_d) is

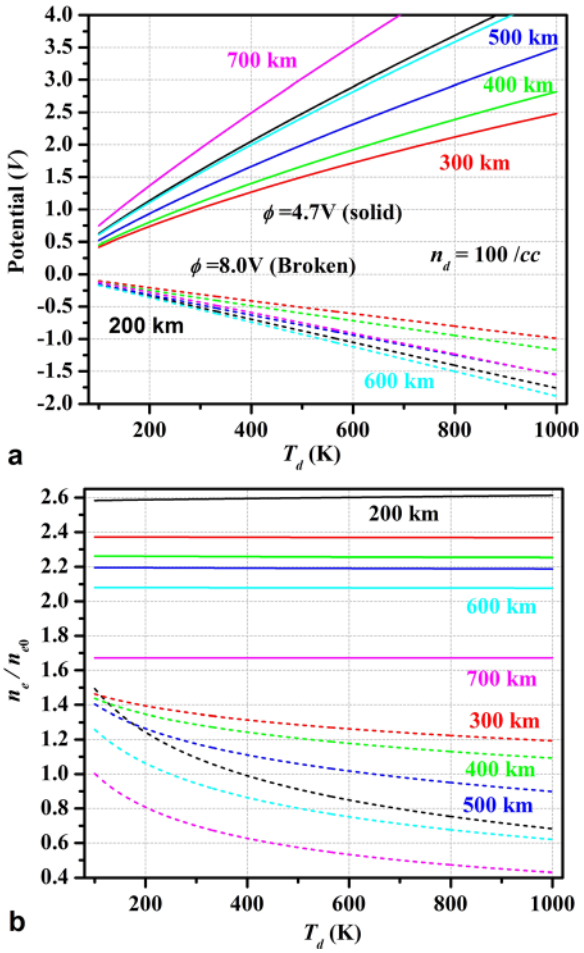

FIG. 7. Steady state dependence of (a) the surface potential over dust particles and (b) dimensionless electron density (n_e/n_{e0}) on the dust surface temperature (T_d) for the parameters $\varphi = 4.7\,\text{eV}$ (CeO_2, solid lines) and $\varphi = 8.0\,\text{eV}$ (pure ice, Broken lines), $n_d = 100/\text{cc}$, $a_o = 0.1\,\mu\text{m}$, and $\chi_m = 1$; the curves correspond to different ionospheric altitudes in the F-layer and the parameter n_e is normalized with its magnitude at referred altitude.

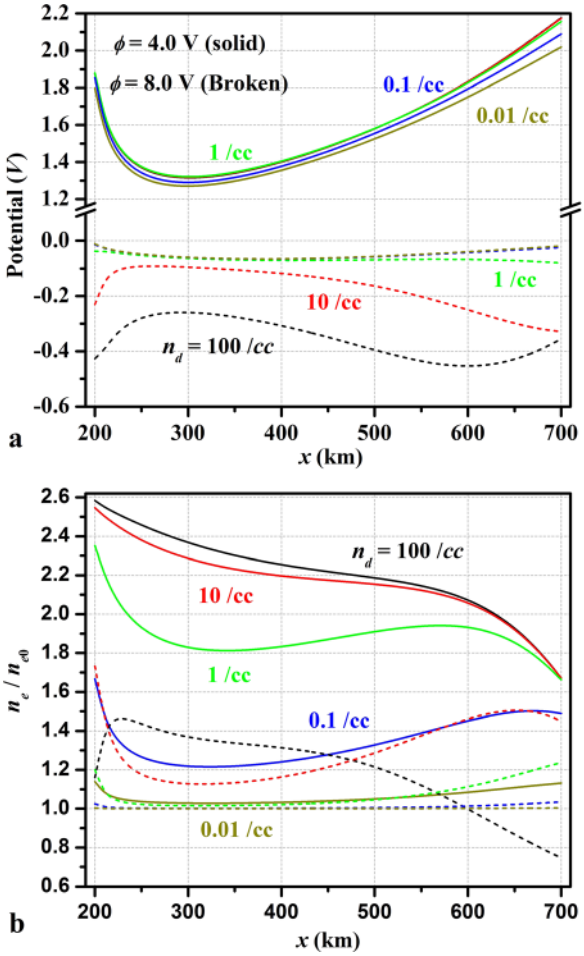

FIG. 8. Steady state dependence of (a) the surface potential over dust particles and (b) dimensionless electron density (n_e/n_{e0}) on the ionospheric altitude (x) for the parameters $\varphi = 4.0\,\text{eV}$ (solid lines) and $\varphi = 8.0\,\text{eV}$ (Broken lines), $a_o = 0.1\,\mu\text{m}$, $T_d = 250\,\text{K}$, and $\chi_m = 1$; the curves correspond to different number densities of the dust particles (n_d) and the parameter n_e is normalized with its magnitude at referred altitude.

illustrated in Fig. 8. The electron density reduction ($n_e/n_{e0} < 1$) is noticed to occur for the large number density and high work function of the dust particles (Fig. 8(b)); usually, the density enhancement is observed for the parameter regime considered herein. The magnitude of the surface potential is noticed to acquire a minimum value around ~300 km altitude (Fig. 8(a)); this is primarily a consequence of large unperturbed (dust free) densities at these altitudes.

Physically, the suspension of the fine dust particles of appropriate work function might lead to the enhancement/decay in the local electron plasma density. Such a density modification may influence the dielectric function (i.e., refractive index/absorption coefficient) of the ionospheric plasma and hence the propagation features of the electromagnetic (em) radiation and radio frequency (RF) signals through the F layer. For instance, the dielectric function of the plasma (with finite collisions) can be expressed as[17] $\varepsilon = [1 - (\omega_{pe}^2/\omega^2)(1 + i\nu/\omega)]$, where $\omega_{pe} = \left(4\pi n_e e^2/m_e\right)^{1/2}$ corresponds to the plasma frequency, ν refers to the collision frequency, and ω is the frequency of the propagating radio/em wave signal which infers the critical plasma density ($n_{cr} = m_e\omega^2/4\pi e^2$). According to this relation, in the unperturbed (dust free) ionospheric region at any given altitude (x), the plasma acts as opaque medium when $\omega \le \omega_{pe0} \Rightarrow n_{cr} \le n_{e0}$ while being transparent for the situation $n_{cr} > n_{e0}$. In the case of plane waves, the refractive index (n) and absorption coefficient (κ) may be correlated with the dielectric function as $(n - i\kappa)^2 = \varepsilon = \varepsilon_r - i\varepsilon_i$, where $\varepsilon_r = (1 - n_e/n_{cr})$ and $\varepsilon_r = (n_e/n_{cr})(\nu/\omega)$. Following Gurevich,[17] the expressions for n and κ corresponding to $\nu_e \ll \omega$ may be approximated as $n \approx \varepsilon_r^{1/2}$ and $\kappa \approx (\varepsilon_i/2n)$, respectively. These relations demonstrate that the reduction in plasma density due to fine particles suspension may lead to the enhanced transparency for the em/RF waves with increasing value of n while the enhancement in the local electron density may improve the opaqueness with higher absorption (κ) resulting in the reflection of the higher RF spectrum. Considering the simple relation of the electron plasma frequency with plasma density, i.e., $\omega_{pe} \propto n_e^{1/2}$, in all the graphical illustrations we have presented the density modification (n_e/n_{e0}). This density modification ultimately affects the dielectric function of the ionospheric plasma and hence n and κ by aforementioned relations. Further, this relation apparently also gives an estimate for the plasma frequency

range. For example, the plasma density may enhance up to ~2.6 times the unperturbed density (Figs. 5–7) which might lead to the local plasma frequency shift to ~1.6 times the unperturbed plasma frequency.

It is also necessary to point out here that we have made computations for selected altitudes in the F layer due to limited access of data and for the sake of simplicity in the analysis and graphical presentation but the conceptual basis is equally applicable to any arbitrary ionospheric altitude. Based on daytime analysis, it is of interest to comment on the effect of dust in the nighttime ionosphere. Although the present analysis/numerical calculations takes account of the midday ionospheric F layer, the conceptual basis is well applicable to the nighttime environment as well. According to Gurevich[17] ionospheric data, the altitude variation of the nighttime electron/ion density is sharp but of smaller value by nearly an order of magnitude with respect to the daytime; this may refer to the smaller diffusion coefficient in the nighttime. Further, in midnight the electron/ion temperature also takes values smaller than that of daytime data. In the absence of the electron emission from fine particles in the nighttime environment (due to the absence of solar radiation which is the dominant source of photoemission in the daytime and weaker field emission effect), the dust particles may acquire only negative potential due to electron/ion accretion. This might lead to electron bite out situation[21] and sufficient reduction in the local plasma density (with respect to ambient) in the presence of the dust particulates; it enhances the transparency for em/RF signal due to lowering of the local electron density; however, the increase in the opaqueness (reflectivity) is difficult in the nighttime due to the absence of significant electron emission.

V. SUMMARY

In summary, a conceptual basis for the ionospheric modification in the midday F region due to artificial insertion of fine dust particulates is formulated. Our formulation includes charging kinetics of the dust particles along with the number and energy balance of the plasma constituents in the F ionospheric region; a novel approach for the inclusion of the electron/ion diffusion in the F layer is considered in this formulation. On the basis of analysis and numerical calculations, the plasma density in these layers is shown to reduce or enhance significantly via inserting the dust particles of high and low work function dust particles, respectively; these effects may further be enhanced by fine tuning of the photoefficiency and surface temperature of the dust particulates. Such density modification locally in the ionospheric plasma layers may influence the transparency/opaqueness of the em/RF waves and can be utilized for appropriate em/RF signal transmission through these layers. In terms of propagation features, the increase in local plasma density refers to decreasing refractive index and enhanced absorption coefficient.[25] The present analysis may be used as a basis to initiate an experimental campaign for improving the radio and satellite communications through the F ionospheric region.

ACKNOWLEDGMENTS

One of the authors (M.S.S.) is grateful to the Department of Science and Technology (DST) for the financial assistance of the work under (Grant No. SR/FTP/PS-215/2011). S.K.M. acknowledges the support from ELI-ALPS project (GINOP-2.3.6-15-2015-00001) which was sponsored by European Union and co-financed by European Regional Development fund. Both the authors are grateful to Dr. Sweta Srivastava for valuable discussion.

[1]T. J. House, J. B. Near, W. B. Shields, R. J. Celentans, D. M. Husband, A. E. Mercer, and J. E. Pugh, "Research paper "Weather as a Force Multiplier: Owning the weather in 2025" Presented to "Air Force 2025"," in *A Symposium on USAF Requirements in 2025* (1996).
[2]P. A. Kossey, AGARD Conf. Proc. **485**, 17A-1 (1990).
[3]K. Davies, *Ionospheric Radio* (Peter Peregrinus Ltd., London, 1990).
[4]V. L. Forlov, N. V. Bakhmet'eva, V. V. Belekovich, G. G. Vertogradov, G. P. Vertogradov, V. G. Komrakov, D. S. Kotik, N. A. Mityakov, S. V. Polyakov, V. O. Rapoport, E. N. Sergeev, E. D. Tereshchenko, A. V. Tolmacheva, V. P. Uryadov, and B. Z. Khudukon, Phys. Usp. **50**, 315 (2007).
[5]L. Spitzer, Astrophys. J. **93**, 369 (1941).
[6]M. S. Sodha, C. J. Palumbo, and J. T. Daley, Br. J. Appl. Phys. **14**, 916 (1963).
[7]M. S. Sodha and S. Guha, "Physics of colloidal plasmas," in *Advances in Plasma Physics*, edited by A. Simon and W. B. Thompson (Interscience Publishers, New York, 1971), Vol. 4, p. 219.
[8]D. A. Mendis, M. Rosenberg, and V. W. Chow, *Physics of Dusty Plasmas* (AIP, New York, 1998).
[9]M. S. Sodha, *Kinetics of Complex Plasmas* (Springer, India, 2014).
[10]M. S. Sodha, S. Misra, and S. K. Mishra, Phys. Plasmas **16**, 123705 (2009); Erratum **17**, 049902 (2010).
[11]S. K. Mishra and S. Misra, Phys. Plasmas **22**, 023706 (2015).
[12]S. Srivastava, R. Mishra, and M. S. Sodha, J. Phys. D: Appl. Phys. **49**, 205503 (2016).
[13]S. J. Bauer, *Physics of Planetary Ionospheres* (Springer, Berlin, 1973).
[14]J. A. Ratcliffe, *Physics of the Upper Atmosphere* (Academic Press, London, 1960).
[15]V. C. A. Ferraro, J. Geophys. Res. **51**, 427, doi:10.1029/TE051i003p00427 (1946).
[16]D. F. Martyn, in *Physics Society. Report on Cambridge Ionospheric Conference* (1955), p. 254.
[17]A. V. Gurevich, *Nonlinear Processes in Ionosphere* (Springer, 1978).
[18]E. W. Mc Daniel, *Collisional Phenomenon in Ionized Gases* (Wiley, New York, 1964).
[19]O. Havnes, T. Aslaksen, and A. Brattli, Phys. Scr. T **89**, 133 (2001).
[20]B. A. Klumov, G. E. Morfill, and S. I. Popel, J. Exp. Theor. Phys. **100**, 152 (2005).
[21]M. S. Sodha, S. Misra, S. K. Mishra, and A. Dixit, Phys. Plasmas **18**, 083708 (2011).
[22]R. H. Fowler, *Statistical Mechanics: The Theory of the Properties of Matter in Equilibrium* (Cambridge University Press, London, 1955).
[23]S. Misra and S. K. Mishra, Mon. Not. R. Astron. Soc. **432**, 2985 (2013).
[24]L. Spitzer, Astrophys. J. **107**, 06 (1948).
[25]M. S. Sodha, S. K. Mishra, and S. K. Agarwal, IEEE Trans. Plasma Sci. **37**, 375 (2009).